Coaxial Pulse Tube Refrigerator for 4K

R. Habibi, M. Thurk, P. Seidel

Institut für Festkörperphysik, Friedrich-Schiller-Universität Jena

ABSTRACT

A pulse tube refrigerator is reported with a coaxial design capable of providing cooling power at 4.2K. The refrigerator features a two-stage design as well as a full coaxial structure. Two needle valves at the hot end of each pulse tube create a valve-controlled active phase shifter. The basic design of our four valve pulse tube refrigerator (FVPTR) has presented previously at other cryocooler conferences[1]. In 2008 this FVPTR achieved a lowest temperature of 5.7K, using a lead-plated mesh in the 2nd regenerator solely. Further tests conducted with this cooler are reported here. The 2nd stage regenerator has been replaced by a three-part combination of lead-coated stainless steel screens and particles of two rare-earth compounds: ErNi0.9Co0.1 and ErNi.

In this setup, a no-load cold tip temperature below 4 K is achievable. The cold tip temperature has been measured for different heat loads to both stages with special attention to 4.2K.

Further the theory of thermodynamics and magnetism predicts a strong proportionality between magnetic heat capacity and the surrounding magnetic field at a given temperature. Therefore the influence of magnetic fields that are higher than that of the earth's magnetic influence on the cooling power was investigated.

INTRODUCTION

The pulse tube refrigerator we were starting from was presented on previous cryocooler conferences[1]. This two-stage cooler was constructed with a coaxial design as Fig. 1 shows. Thereby, the horizontal mechanical vibrations are reduced. The main inlets and outlets of the pulse tubes are connected periodically to the high- or low-pressure side of a commercial helium-compressor (Leybold RW 6000, nominal input power 7 kW). An active phase shift between the volume and the pressure is provided by the valve control unit with two needle valves at each regenerator. The 1st stage regenerator has been made of stainless steel wire mesh screens and the 2nd stage regenerator has been made of lead coated wire mesh screens. Lead has been used because it has a high volumetric heat capacity from the phonon system below 50K. With this configuration and some additional flow diffuser improvements, a no-load cold tip temperature of 5.7K was achieved. That seems to be the physical limit of the regenerator made of lead coated sieves. Therefore, another approach is necessary.

The volumetric heat from the phonon system decreases in the third order of temperature as by the Debye-theory predicted. This means that thermal regeneration below 10K is fairly ineffective. Hence the temperature gradient at the regenerator is small in this level of temperature. In order to gain a more effective regeneration it is well known that entropy must be provided from one that is different from the phonon system. Magnetic phase transitions of rare-

Cryocoolers 17, edited by S.D. Miller and R.G. Ross, Jr.

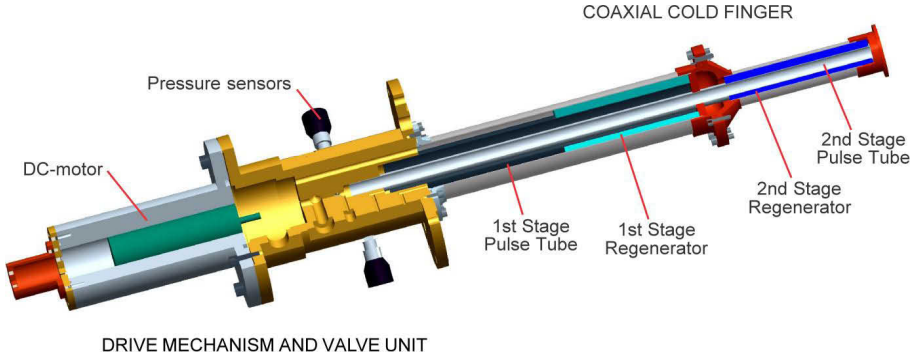

Figure 1. Layout of the two-staged FVPTR. The pulse tubes are located inside the respective regenerators. Additionally, the 2nd stage pulse tube is placed at the centerline of the 1st stage pulse tube. Therefore, a ring-shaped space for the 1st stage pulse tube occurs.

earth compounds have been used to generate a large change in entropy in this temperature range for many years[2]. Hence we have used two of these materials for the regenerator in the 2nd stage as well.

With the aim to demonstrate the ability of the coaxial design to liquefy helium which means to reach cooling power at 4.2K, the temperature profile of the 2nd stage was measured for the planned optimization. The regeneration is ineffective below 10K as it leads to a small temperature gradient for large parts of the regenerator. A consequence of this result is that materials with a magnetic phase transition should be used in the 2nd stage regenerator.

EXPERIMENTAL SET-UP

Preliminary Investigations

In order to measure the temperature profile of the 2nd stage we have placed LakeShore DT-470 sensors along the regenerator. The cold tip temperature was measured with a calibrated LakeShore CX-1030 sensor for higher precision.

We planned to use ErNi and ErNi0.9Co0.1 in the regenerator. Optical microscope images of these materials are shown in Fig. 2. To get an estimate of the flow resistances of these two different shapes, a pressure loss measuring system (see Fig. 3a) was built. A high precision is attainable by measuring the pressure loss directly with one sensor. Furthermore, mechanisms have been tested with the same device to avoid any leakage of the rare-earth particles (Fig. 3b).

Three sensors with maximum ranges of 0.1 bar, 0.5 bar and 2.5 bar have been used (MPX 5010DP, MPX 5050DP and MPX 4250DP, Freescale) for the differential pressure measurement.

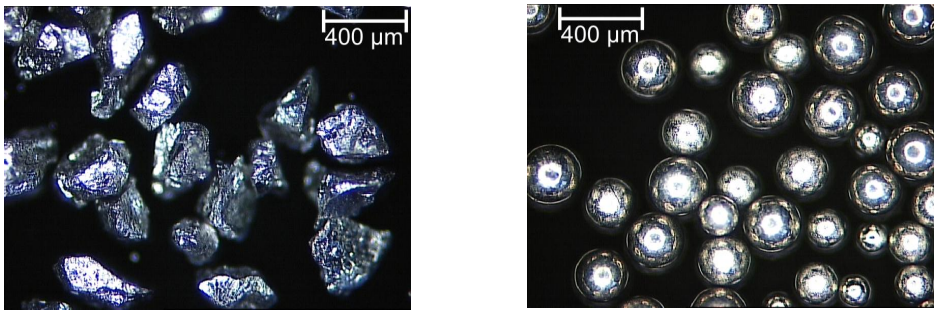

Figure 2. Optical microscope images of $ErNi_{0.9}Co_{0.1}$ grains (left) and ErNi spheres (right) with diameters from 150 µm up to 300 µm.

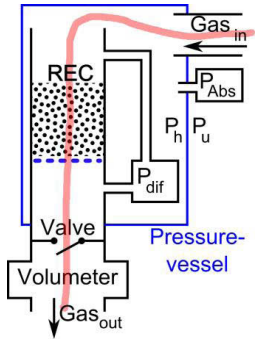

Figure 3a. Construction for pressure loss measurement. The rare-earth compound in the pipe causes a pressure loss that depends on the absolute pressure and on the volume flow.

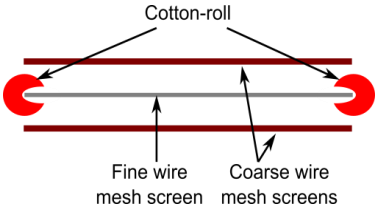

Figure 3b. Construction to avoid leakage of rare-earth particles.

We have used a vibrating sample magnetometer to measure susceptibility versus temperature to prove that the rare-earth compounds perform a magnetic phase transition. This device magnetizes a vibrating sample by large coils. A time dependent magnetic field is induced in the pickup coils due to the movement of the magnetized sample. This device can provide magnetic fields up to 2 T.

Second Stage Regenerator

The 2nd stage was reconstructed with a 17 % increased length for necessary devices to contain the regenerator particles. The layout of the multilayer 2nd stage regenerator is schematically shown in Fig. 4. Table 1 lists the detailed amount of material in each layer. An ohmic resistor has been attached at the cold end of each stage to simulate different heat loads to measure the cooling power characteristics.

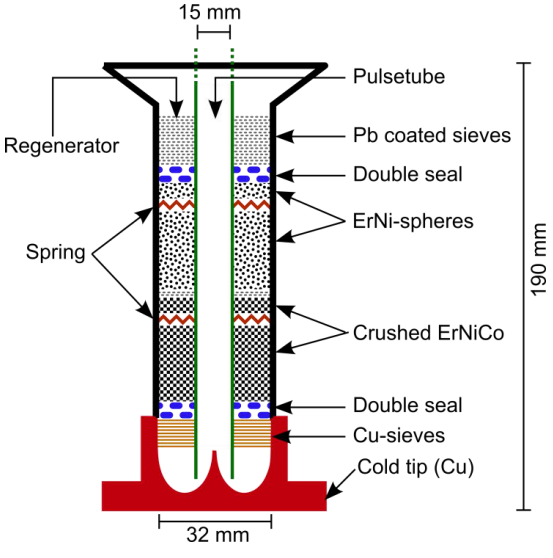

Figure 4. Schematic view of the 2nd stage. $ErNi_{0.9}Co_{0.1}$ is used for regeneration at the cold tip. The ErNi is placed in the middle section because the maximum of its volumetric heat occurs at higher temperatures. Near the warm end we reused the Pb coated sieves.

Table 1. Length proportion and mass of total regenerator length for each used material.

Material	Proportion of total regenerator length [%]	Mass [g]
$ErNi_{0.9}Co_{0.1}$	40	194
ErNi	33	192
Pb coated sieves	27	-

Two parallel arranged permanent magnets at room temperature provide a higher external magnetic field (dimensions of magnets: 111mm x 89mm x 20mm, distance: 97mm). The 2nd stage cold finger has been placed between them to investigate the influence of static external magnetic fields. Thereby the field around the regenerator varies from 60 mT at the edges to 130 mT in the center. Temperature measurement in this configuration is only precise with magnetic field insensitive Cernox sensors.

EXPERIMENTAL RESULTS AND DISCUSSION

Preliminary Investigations

Figure 5 illustrates that regeneration below 10K is ineffective with a regenerator made ony of lead. Replacing the materials in the regenerator by other ones will influence the temperature profile. Since we cannot define the axial position of each material transition with high accuracy, we have used these results for a rough reference for the material distribution. Simple calculations from the regenerator theory of H. Hausen have confirmed this approximation[3].

Investigation by Radebaugh about the volumetric heat capacities of different rare-earth compounds gave us an orientation for choosing suitable magnetic regenerator materials[4]. With the aim of providing high cooling power at 4.2K, the compounds GOS (Gd2O2S) at the cold tip and ErNi or ErNi0.9Co0.1 for regions above 6K are suitable. Finally crushed ErNi0.9Co0.1 and ErNi spheres with a diameter range of 150 µm up to 300 µm has been used. Together with lead coated wires, the regenerator has a three component design. The local maximum of the volumetric heat of ErNi0.9Co0.1 occurs at a slightly lower temperature. Hence it should be used at the cold end. The lead coated wire mesh screens are suited well for regeneration above 15K.

The flow behavior has been investigated first because of the different shape of the rare-earth compounds. Figure 5a shows that the pressure losses for both materials are equivalent. This effect may be caused by a different porosity which means that the volume flow has a higher cross-section area and a lower velocity. Such a good compliance in flow resistance makes the materials suitable for simultaneous usage in the regenerator because none of them will limit the maximum volume flow alone. One can expect that the compressor consumption power will increase: higher losses generate higher pressure ratio between the inlet and the outlet pressure of the compressor.

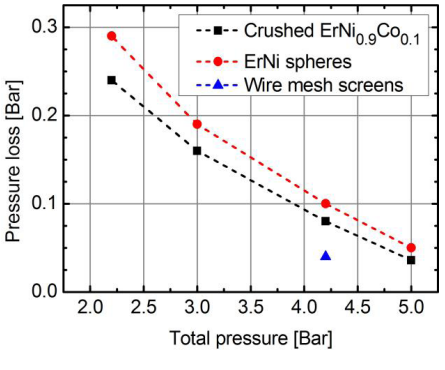

Figure 5a. Pressure loss for $ErNi_{0.9}Co_{0.1}$, ErNi and the previous Pb coated sieves.

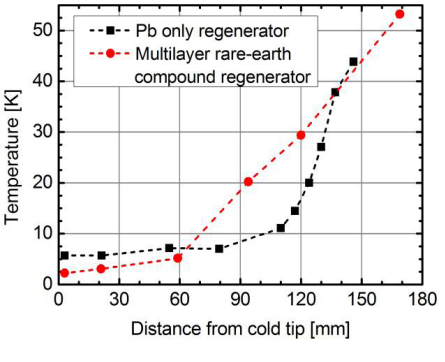

Figure 5b. Axial temperature profile of the improved and of the previous 2nd stage.

If a regenerator contains small particles, a containment mechanism to avoid particle leakage ("seals") will be necessary. At first a thin cotton layer between the two coarse mesh wire screens had been tested for this purpose but even a very thin layer produces a pressure loss of more than 2.5 bar at typical volume flows. Therefore another design (Fig. 3b) has been used. With this construction no leakage occured. The cotton has been used only for the contact between the regenerator and the containment wall to seal the ragged wire mesh screens. So the pressure loss can be neglected (loss < 10 mbar at 2.2 bar absolute pressure).

The magnetic phase transition is recognizable in the diagram from the magnetometer (Fig. 6a). For an empty sample the magnetization is below the resolution limit for all values of external magnetic fields. By using samples containing the magnetic materials a strong temperature dependence of the magnetization could be observed. The absolute value of the magnetization increases when the temperature decreases. From these data the magnetic part of the specific heat can be calculated in intervals (Fig. 7b). For the calculation the formula for the heat capacity from the magnetic system has been used: (B: surrounding magnetic field, M: Magnetization, T: Temperature.)

$$c_{magnetic} = -B\,\frac{dM}{dT} \tag{1}$$

We have measured the highest magnetic heat capacity between 4K and 8K. The value around 5K is 28 times larger than at 17 K. Thus the change in susceptibility at low temperatures is proved.

Cooling Power of the Refrigerator

The cooling power characteristic of the cooler is given in Fig. 7. The no-load temperature is 2.41K. At 4.2K a cooling power of 320 mW is provided which means a Carnot-efficiency of 0.26 %. In comparison to the refrigerator we started with the 1st stage temperature has slightly increased. This is caused by the higher gas volume that is stored in the 2nd stage. That is not available as a working fluid in the 1st stage. As mentioned before an increase in the compressor consumption power from 6.2 kW to 8.3 kW occurs. The optimal working frequency for this design is 2.34 Hz.

The temperature profile has changed significantly (Fig. 5b). The regenerator in multilayer design is capable of providing a high temperature gradient over two-thirds of its length. The thermally active part of the regenerator is doubled in contrast to the lead-only regenerator.

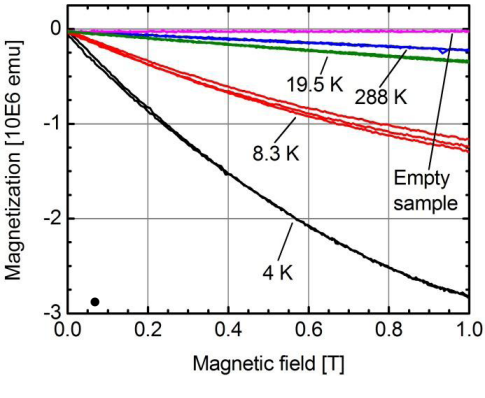

Figure 6a. Vibrating sample magnetometer diagram shows temperature dependence of the susceptibility.

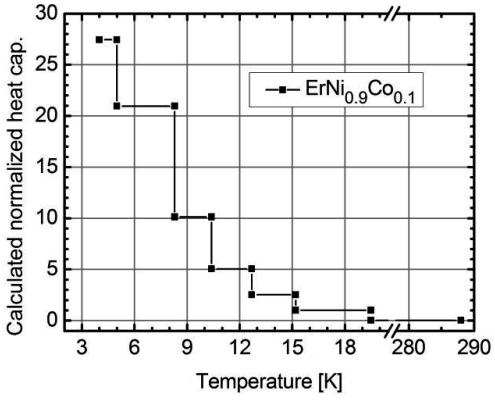

Figure 6b. Various normalized calculated heat capacity from the magnetic system.

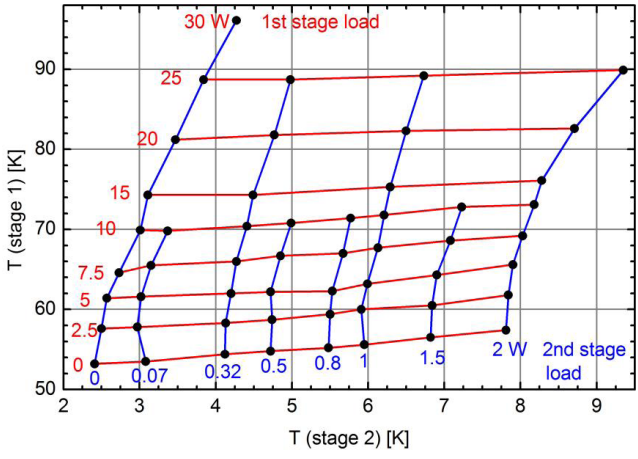

Figure 7. Cooling power characteristic of the FVPTR for 4 K.

External Magnetic Field

Using an external magnetic field, the theory of thermodynamics predicts an additional part of the heat capacity according to Eq.1. A high heat capacity can be obtained in the region of the Curie-temperature respectively of the Neél-temperature. In this region, a large change in susceptibility can be expected. Furthermore, Eq. 1 predicts a proportionality between heat capacity from the magnetic system and the external magnetic field. In normal operation mode, the external magnetic field only comes from the earth. Higher fields are realizable by permanent magnets installed around the cold finger. The heat capacity should increase with an increase of the magnetic field[5]. Our permanent magnets generate a magnetic field three orders of magnitude larger than the earth's magnetic field. However measurements of the cooling power versus temperature have not shown any increase in cooler performance. This result makes a further investigation necessary.

CONCLUSION

In order to provide cooling power at 4.2K we have improved the heat transfer capability of the low temperature regenerator using an arrangement of ErNi0.9Co0.1 spheres and ErNi grains as well as lead coated wire mesh screens.

We have demonstrated that a two staged pulse tube refrigerator with a coaxial design is capable of providing cooling power at 4.2K.

REFERENCES

1. Köttig, T., Nawrodt, R., Thürk, M., and Seidel, P., "Performance Characteristic of a Two-Stage Pulse Tube Refrigerator in Coaxial Configuration," *Cryocoolers 14*, ICC Press, Boulder (2007), pp. 171-176.
2. Nagano, M., Inaguchi, T., Yoshimura, H., Yamada, T., Iwamoto, M., "Helium Liquefaction by a Gifford-McMahon Cycle Cryocooler," *Adv. in Cryogenic Engineering,* Vol. 37B, Plenum Publishing Corp., New York (1992), pp. 1251-1260.
3. Hausen, H., Linde, H., *Tieftemperaturtechnologie, Vol. 2*, Springer, Berlin (1985), pp. 169-183.
4. Radebaugh, R., Huang, Y., O'Gallagher, A., and Gary, J., "Calculated Performance of Low-Porosity Regenerators at 4 K with He-4 and He-3," *Cryocoolers 15*, ICC Press, Boulder (2009), pp. 325-334.
5. Bischof, J., Divis, M., Svoboda, P., and Smetana, Z., "The Specific Heat of HoCu2 in Magnetic Fields," *Phys. Stat. Sol.*, Vol. 114, Prague (1989), pp. 229-231.